

# New Polyether Macrocycles as Promising Antitumor Agents—Targeted Synthesis and Induction of Mitochondrial Apoptosis

Ilgiz I. Islamov,\* Lilya U. Dzhemileva,\* Ilgam V. Gaisin, Usein M. Dzhemilev, and Vladimir A. D'yakonov



Cite This: *ACS Omega* 2024, 9, 19923–19931



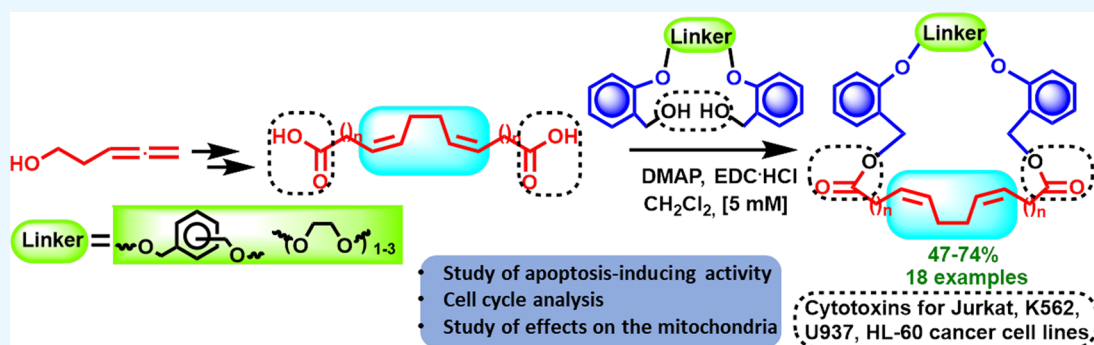
Read Online

ACCESS |

Metrics & More

Article Recommendations

Supporting Information



**ABSTRACT:** A series of previously unknown aromatic polyether macrodiolides containing a *cis,cis*-1,5-diene moiety in the molecule were synthesized in 47–74% yields. Macrocycle compounds were first obtained by intermolecular esterification of aromatic polyether diols with  $\alpha,\omega$ -alka- $nZ,(n+4)Z$ -dienedioic acids mediated by *N*-(3-(dimethylamino)propyl)-*N'*-ethylcarbodiimide hydrochloride (EDC·HCl) and 4-(dimethylamino)pyridine (DMAP). For the synthesized compounds, studies of cytotoxicity on tumor (Jurkat, K562, U937), conditionally normal (HEK293) cell lines, and normal fibroblasts were carried out. CC50 was determined, and the therapeutic selectivity index of cytotoxic action (SI) in comparison with normal fibroblasts was evaluated. With the involvement of modern methods of flow cytometry for the most promising macrocycles, their effect on mitochondria and the cell cycle was investigated. It was found that a new macrocycle exhibits pronounced apoptosis-inducing activity toward Jurkat cells and can retard cell division by blocking at the G1/S checkpoint. Also, it was shown that the synthesized macrodiolides influence mitochondria due to their high ability to penetrate the mitochondrial membrane.

## INTRODUCTION

The large diversity of macrocyclic compounds in nature and the broad range of useful properties they exhibit have always attracted researchers to work in various areas. Currently, quite a number of macrocycles are used in pharmaceuticals,<sup>1</sup> materials science, supramolecular chemistry,<sup>2–5</sup> and catalysis.<sup>6–10</sup>

Strained macrocycles, including cyclophanes, are of special interest. Owing to their rigid structure and stable configuration, these compounds can be used in medicinal chemistry as both full-value biologically active substances and bases for the development of highly efficient systems for drug delivery to biological targets.<sup>1</sup> Antitumor, antiviral, antibacterial, and fungicidal properties were found for numerous natural and synthetic cyclophane derivatives.<sup>11–14</sup>

Since 1967, when Pedersen reported the synthesis and study of properties of a new class of polyether macrocyclic compounds,<sup>15,16</sup> called crown ethers, the research interest in this class of macrocycles has been steadily growing. Today, these polyether macrocycles represent groups of compounds

that, apart from their high versatility and broad use in chemistry and industry, could also find biomedical applications as modern effective antibacterial and antitumor agents.<sup>17–22</sup>

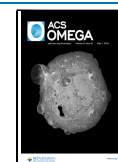
Important features determining the biological activity of crown ethers are high lipophilicity, selectivity of complex formation, and the ability to transport ions and some neutral molecules across biological membranes, similar to natural ionophores. Owing to these properties, the indicated macrocycles are rather often utilized for targeted delivery of antitumor and antimicrobial agents and polyfunctional molecules exhibiting multitarget properties. Polyether macro-

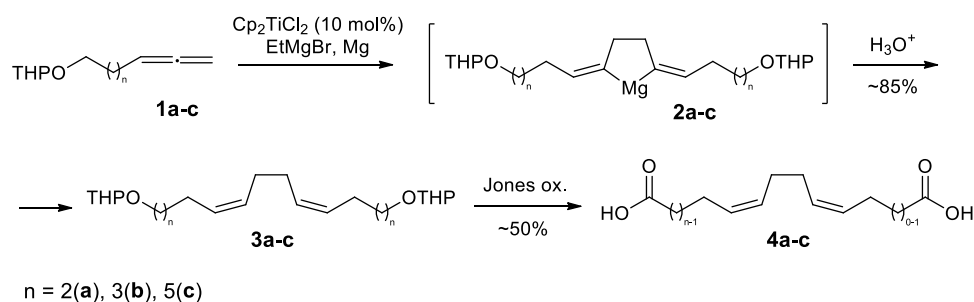
Received: November 30, 2023

Revised: April 9, 2024

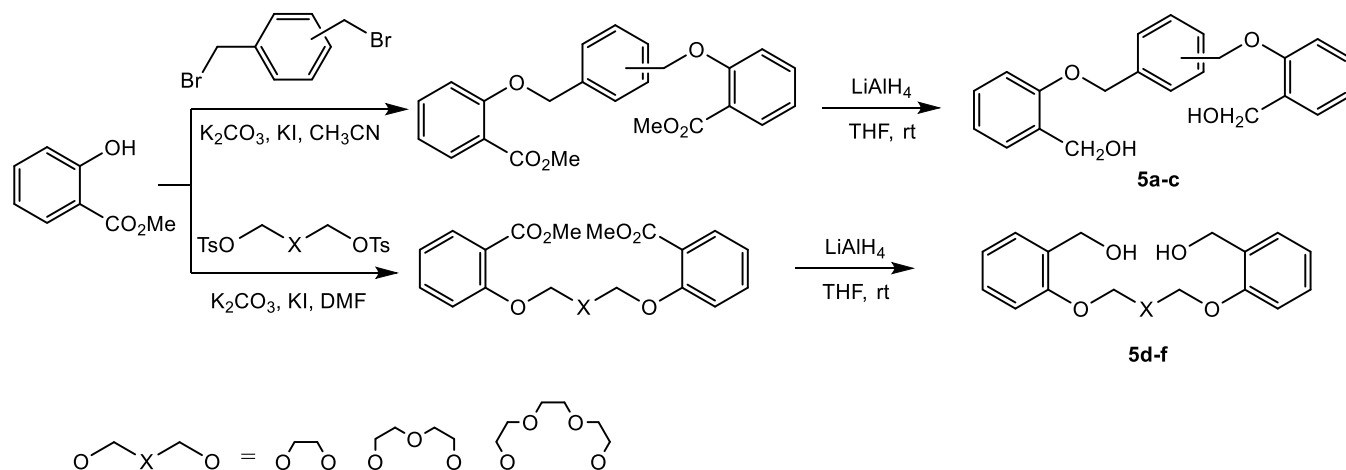
Accepted: April 18, 2024

Published: April 29, 2024



Scheme 1. Synthesis of  $\alpha,\omega$ -Alka- $nZ,(n + 4)Z$ -dienedioic Acids 4a–c

## Scheme 2. Synthesis of Aromatic Diols 5a–f



cycles can affect the enzymatic activity, interact with DNA, cleave DNA, and also act as antibacterial agents.<sup>23–29</sup>

In addition, these polyether macrocycles are attractive as molecular scaffolds for the preparation of hybrid compounds by the introduction of known pharmacophore fragments into the molecules, which may give rise to new products with high biological activities.

It is known that the 1*Z*,5*Z*-diene moiety is encountered in numerous biologically active compounds, for example, fatty 5*Z*,9*Z*-dienoic acids, leimbeynes, acetogenins, and insect pheromones.<sup>30</sup> Our previous studies were related to the development of efficient stereoselective syntheses of *cis,cis*-unsaturated natural and synthetic compounds, which exhibit antitumor, antibacterial, and neurotogenic properties.<sup>31–33</sup>

Previously, we showed that macrocycles with a 1*Z*,5*Z*-diene moiety possess *in vitro* cytotoxicity against some tumor cell lines. The highest activity against T-cell leukemia (Jurkat), chronic myeloid leukemia (K562), histiocytic lymphoma (U937), and cervical cancer (HeLa) cells was found for macrodiolides that contained an aromatic moiety in the molecule ( $CC_{50} = 0.04\text{--}0.17\ \mu\text{M}$ ). The subsequent studies demonstrated that, being inducers of programmed cell death, macrodiolides initiate apoptosis in Jurkat cells by the mitochondrial pathway and suppress the growth and proliferative activity of tumor cells by inhibiting Akt, p38, and CREB kinases.<sup>34</sup>

In view of the above, we intended to continue the research aimed at the stereoselective synthesis of *cis,cis*-unsaturated macrocyclic compounds, the study of their cytotoxicity, and the exploration of the relationship between the structure and antitumor activity of the macromolecules. In particular, it was of interest to synthesize macrocyclic compounds, crown ether

derivatives, which contain both aromatic and mono-, di-, and triethylene glycol moieties, and to carry out comparative analysis of their antitumor properties.

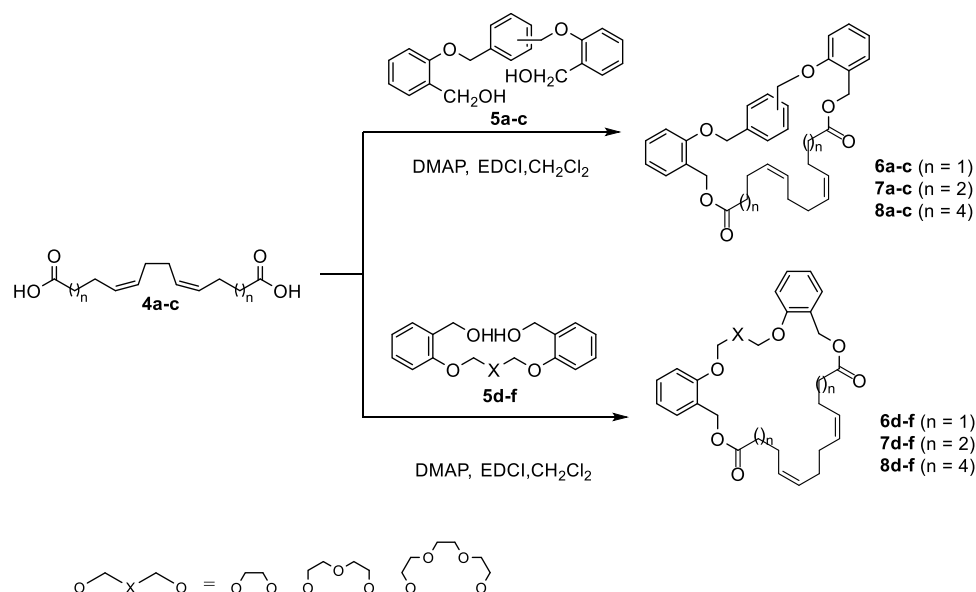
## RESULTS AND DISCUSSION

It is known that high potential for the development of antitumor drugs is inherent in fatty unsaturated acids with different chain lengths between the 1*Z*,5*Z*-diene moiety and the carboxyl group and in various  $\alpha,\omega$ -alka- $nZ,(n + 4)Z$ -dienedioic acid derivatives, which inhibit human topoisomerases I and II when present in low concentrations and also have cytotoxic activity against some cancer cell lines.<sup>35,36</sup> In view of the above, we synthesized the target macrocycles by the cyclocondensation of  $\alpha,\omega$ -alka- $nZ,(n + 4)Z$ -dienedioic acids with various aromatic diols.

The key diene precursors (1,12-dodeca-4*Z*,8*Z*-dienedioic acid (**4a**), 1,14-tetradeca-5*Z*,9*Z*-dienedioic acid (**4b**), and 1,18-octadeca-7*Z*,11*Z*-dienedioic acid (**4c**)) were synthesized in ~43–46% yields by a previously developed three-step route using homocyclomagnesiation reaction of O-containing 1,2-dienes (Scheme 1).<sup>34</sup>

It is known that macrocyclization of  $\alpha,\omega$ -alka- $nZ,(n + 4)Z$ -dienedioic acids with aromatic compounds in which the hydroxyl group is directly bound to the aromatic ring (dihydroxybenzenes, naphthalenediols) gives products in very low yields.<sup>34</sup> Meanwhile, we ascertained that the separation of the hydroxyl group from the ring, even by one methylene unit, substantially facilitates macrocyclization and increases the yields of products. Therefore, in this study, for the synthesis of target polyether cyclophanes, we prepared aromatic diols in which the functional groups were separated from the aromatic ring. The reactions of dibromoxylenes (*o*-dibromoxylene, *m*-

Scheme 3. Synthesis of Polyether Macrocycles 6–8



Diacid	Diol	Macrocycle	Yield (%)
4a	5a	6a	49
4a	5b	6b	56
4a	5c	6c	60
4a	5d	6d	47
4a	5e	6e	58
4a	5f	6f	62
4b	5a	7a	54
4b	5b	7b	58
4b	5c	7c	67
4b	5d	7d	53
4b	5e	7e	60
4b	5f	7f	67
4c	5a	8a	55
4c	5b	8b	60
4c	5c	8c	74
4c	5d	8d	55
4c	5e	8e	69
4c	5f	8f	72

dibromoxylene, and *p*-dibromoxylene) with methyl salicylate in the presence of  $\text{K}_2\text{CO}_3$  gave their derivatives as esters.<sup>37</sup> Then, the ester group was reduced with  $\text{LiAlH}_4$  in THF, thus furnishing the target aromatic diols **5a–c** (Scheme 2). Target polyether aromatic diols **5d–f** were obtained by a similar route starting from ethylene glycol ditosylates and methyl salicylate with subsequent transformations (Scheme 2).<sup>37</sup>

While addressing the final stage of the synthesis of the target macrocycles, we first tested the intermolecular macrolactonization induced by catalytic amounts of transition metal triflates.<sup>38,39</sup> However, despite all our efforts toward the development of optimal conditions, the yields of the target macrocycles were less than 30%. Meanwhile, the use of macrocyclization reaction involving carbodiimides proved to be fairly successful.<sup>40</sup> As a result, by cyclocondensation of  $\alpha,\omega$ -alka-*nZ*,(*n* + 4)*Z*-dienedioic acids and polyether aromatic diols in the presence of DMAP and EDCI, we synthesized previously unknown polyether macrocycles in 47–74% yields (Scheme 3).

Under the conditions we developed earlier,<sup>40</sup> at a molar ratio of reagents diacid (**4**)/diol (**5**)/DMAP/EDCI = 1:1:0.5:2 with strong dilution in dichloromethane ([5 mM]), the reaction proceeds with the formation of a single product (adduct 1:1 cycloaddition). The yields of the reactions varied according to definite patterns and increased in the series of diols from **5a** to **5c** and also in the series from **5d** to **5f**. Furthermore, the yields increased with increasing hydrocarbon chain length in dienedicarboxylic acid from **4a** to **4c**. Indeed, the reaction of 1,12-dodeca-4*Z*,8*Z*-dienedioic acid **4a** with diol **5a** afforded the target cyclophane in 49% yield, whereas the reaction of 1,18-octadeca-7*Z*,11*Z*-dienedioic acid **4c** with diol **5c** gave the product in 74% yield (Scheme 3).

The structure of the synthesized macrocycles **6–8** was established by high-resolution mass spectrometry,  $^1\text{H}$  and  $^{13}\text{C}$  NMR spectroscopy, and heteronuclear two-dimensional (2D) correlation experiments (HSQC, HMBC).

Previously, it was found that crown ether compounds can inhibit tumor cell growth by disrupting potassium ion

**Table 1. Cytotoxic Activities In Vitro of Synthesized Macrocycles 6–8 Measured on Cell Cultures (Jurkat, K562, U937, Hek293, and Normal Fibroblasts) ( $\mu\text{M}$ )**

Comp.	Jurkat ( $\text{CC}_{50}\mu\text{M}$ ) <sup>a</sup>	K562 ( $\text{CC}_{50}\mu\text{M}$ ) <sup>a</sup>	U937 ( $\text{CC}_{50}\mu\text{M}$ ) <sup>a</sup>	Hek293 ( $\text{CC}_{50}\mu\text{M}$ ) <sup>a</sup>	Fibrobl. ( $\text{CC}_{50}\mu\text{M}$ ) <sup>a</sup>	selectivity Index	$\text{CC}_{50\text{max}}/\text{CC}_{50\text{min}}$
5a	1.69 ± 0.18	1.98 ± 0.21	1.76 ± 0.17	7.88 ± 0.81	9.24 ± 0.95	1.69–9.24	4.71
5b	1.84 ± 0.19	2.27 ± 0.24	1.97 ± 0.19	8.19 ± 0.84	9.83 ± 0.98	1.84–9.83	5.34
5c	2.96 ± 0.31	3.34 ± 0.35	2.84 ± 0.27	10.47 ± 1.12	12.67 ± 1.36	2.96–12.67	4.28
6a	0.19 ± 0.02	0.17 ± 0.03	0.11 ± 0.02	1.84 ± 0.19	3.08 ± 0.34	0.19–3.08	16.21
6b	0.15 ± 0.01	0.19 ± 0.02	0.17 ± 0.01	1.61 ± 0.17	2.73 ± 0.28	0.15–2.73	18.20
6c	0.61 ± 0.05	0.39 ± 0.03	0.49 ± 0.04	2.57 ± 0.27	3.82 ± 0.37	0.39–3.82	9.79
6d	2.04 ± 0.21	2.57 ± 0.25	1.98 ± 0.19	8.91 ± 0.92	10.68 ± 1.05	1.98–10.68	5.39
6e	2.57 ± 0.25	2.98 ± 0.28	2.39 ± 0.23	9.47 ± 0.96	11.37 ± 1.24	2.39–11.37	4.75
6f	2.78 ± 0.28	3.24 ± 0.32	2.59 ± 0.26	9.93 ± 1.02	12.09 ± 1.31	2.59–12.09	4.66
7a	0.21 ± 0.02	0.16 ± 0.03	0.14 ± 0.01	1.91 ± 0.21	2.98 ± 0.31	0.21–2.98	14.19
7b	0.17 ± 0.02	0.22 ± 0.02	0.19 ± 0.02	1.86 ± 0.19	2.69 ± 0.26	0.17–2.69	15.82
7c	0.67 ± 0.07	0.41 ± 0.04	0.47 ± 0.04	2.84 ± 0.28	3.72 ± 0.36	0.41–3.72	9.07
7d	2.12 ± 0.22	2.49 ± 0.24	2.02 ± 0.18	9.07 ± 0.91	10.11 ± 1.01	2.02–10.11	5.00
7e	2.49 ± 0.24	3.02 ± 0.31	2.44 ± 0.25	9.51 ± 0.93	11.59 ± 1.19	2.44–11.59	4.75
7f	2.81 ± 0.29	3.18 ± 0.30	2.74 ± 0.28	9.28 ± 0.93	11.24 ± 1.26	2.74–11.24	4.10
8a	0.20 ± 0.02	0.18 ± 0.02	0.12 ± 0.01	1.86 ± 0.19	2.74 ± 0.28	0.12–2.74	22.83
8b	0.18 ± 0.02	0.20 ± 0.02	0.17 ± 0.03	1.79 ± 0.17	2.93 ± 0.30	0.18–2.93	16.27
8c	0.59 ± 0.08	0.44 ± 0.05	0.42 ± 0.04	2.79 ± 0.29	3.89 ± 0.37	0.42–3.89	9.26
8d	2.31 ± 0.23	2.51 ± 0.25	2.06 ± 0.19	8.95 ± 0.90	11.23 ± 1.27	2.06–11.23	5.45
8e	2.61 ± 0.26	3.17 ± 0.33	2.59 ± 0.26	9.81 ± 1.01	12.07 ± 1.29	2.59–12.07	4.66
8f	2.89 ± 0.29	3.12 ± 0.31	2.81 ± 0.28	9.93 ± 0.97	12.04 ± 1.21	2.81–12.04	4.28
staurosporin	1.72 ± 0.15	4.35 ± 0.85	3.77 ± 0.54	8.16 ± 0.88	18.08 ± 2.12	1.72–18.08	10.51

<sup>a</sup>Data are presented as the mean  $\pm$  SEM calculated from the results of at least 3 independent experiments.

homeostasis, which, in turn, leads to cell cycle disruption and apoptosis.<sup>19</sup> In order to expand the library of polyether macrocycles with antitumor activity and assess their potential clinical applicability, we studied the products for *in vitro* cytotoxicity and the ability to affect the cell cycle and induce apoptosis (Table 1).

The choice of cell lines for the cytotoxicity studies is not random. We are actively studying the effect of various compounds specifically on hemoblastosis cells. Therefore, all of the cell lines we selected (Jurkat, K562, U937) are different types of hemoblastosis. The HEK293 line is a conditionally normal cell line; fibroblasts were taken into the study as control healthy cells to calculate the selectivity index.

The results of cytotoxicity assays of the prepared macrodiolides using tumor cells (Jurkat, K562, U937), conditionally normal cells (Hek293), and normal fibroblasts provide the following conclusions (Table 1):

- the cytotoxicity of macrodiolides (6a–c)-(8a–c) against any of the used cells markedly exceeds the cytotoxicity of the initial aromatic diols 5a–c; the most pronounced cytotoxicity in this series of compounds is inherent in macrodiolides based on *ortho*- and *meta*-isomers;
- the introduction of one, two, or three ethylene glycol moieties into macrodiolide molecules, instead of the central benzene moiety of the aromatic diol, leads to a pronounced decrease in the cytotoxicity of macrodiolides (6d–f)-(8d–f);
- the cytotoxicity of all macrodiolides was shown to barely change with increasing number of methylene units in the moiety formed by dienedicarboxylic acids 4a–c; and
- the selectivity index (SI) of the cytotoxic action of the macrodiolides is 3–9 for conditionally normal human embryonic kidney cells (Hek293) and 4–28 for normal fibroblasts.

The most active compounds 6a–c were chosen for subsequent studies of the induction of apoptosis, the effect on the cell cycle, and the possible mechanism of the cytotoxic action.

We analyzed the selectivity index of the synthesized compounds (Table 1). The table shows that there is a certain pattern in the cytotoxicity of compounds, depending on their chemical structure. To study the effect on mitochondria, we selected a group of compounds 6a–6c as compounds with some average difference between the highest toxic concentration values in normal cells and the lowest CC50 value in a tumor culture. For all biological experiments, we performed three independent experiments. Jurkat is a T-cell leukemia, U937 is a histiocytic lymphoma cell, and K562 is an immortalized myelogenous leukemia. A study of apoptosis together with damage to mitochondria and the cell cycle was performed on the P53-deficient cell line Jurkat for the purpose of ensuring that the internal p53-dependent apoptosis pathway is turned off in the cells.

We studied new compounds as inducers of apoptosis and their effects on the cell cycle. Apoptosis and mitochondrial damage were studied by flow cytometry using annexin V, mitochondrial dye X-red, and 7-aminoactinomycin D (7AAD) (Millipore, Bedford, MA). If cells positive for h-red and negative for other dyes were detected in the cells, then we defined them as living since the mitochondrial dye h-red is a vital dye. Apoptotic cells are characterized by the externalization of phospholipid phosphatidylserine (PS), which is normally located on the inner surface of the cell membrane in living cells. The arrangement of phospholipids on the outer surface of the membrane can be detected from early apoptosis to complete cell degradation. Thus, the use of recombinant annexin V protein, which exhibits a high affinity for phosphatidylserine, conjugated with the fluorescent dye Alexa

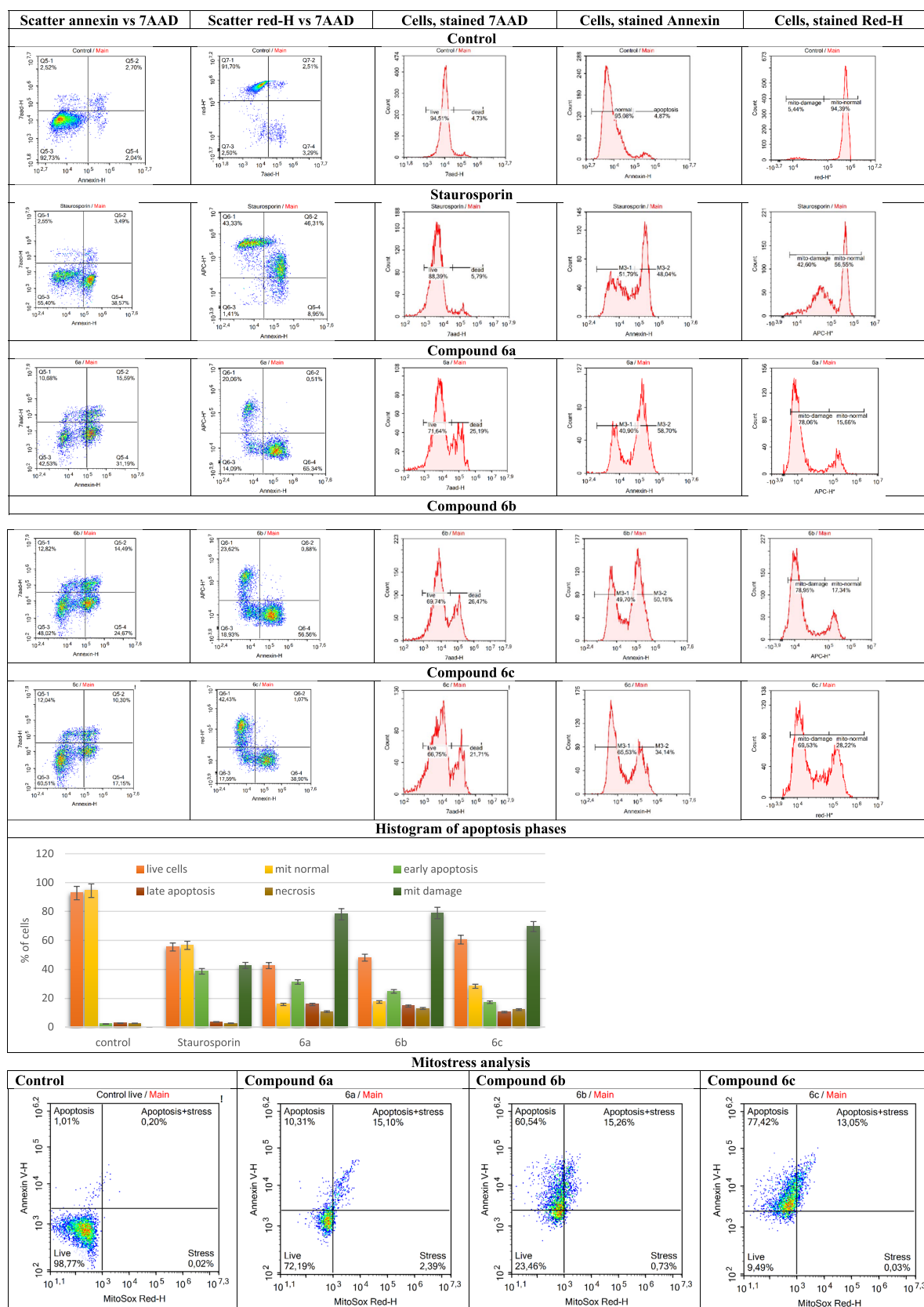


**Figure 1.** Detection of apoptosis caused by the change in the mitochondrial potential ( $\Delta\Psi$ ) in Jurkat cells treated with compounds **6a**, **6b**, and **6c** at concentrations of 1.5 CC50. The control sample contained untreated live cells; overall histogram of the phases of apoptosis with allowance for the cells with damaged mitochondria. The cells treated with staurosporine at a concentration of 0.2  $\mu\text{M}$  served as the positive control. The cells were stained with MitoSense Red, annexin V-CF488A, and 7-AAD. The incubation time was 4 h. Detection of ROS ion production under the influence of the studied compounds in Jurkat culture cells. The incubation time was 4 h. Cell cycle phases for Jurkat cells treated with compounds **6a**, **6b**, and **6c** at CC50 concentration. The incubation time of compounds with the cells was 24 h.

Fluor 488, makes it possible to detect cell apoptosis with high accuracy. The use of annexin V in combination with 7AAD and h-red allows simultaneous discrimination between viable cells ( $V-/7AAD \mp h\text{-red}$ ), early apoptotic cells ( $V+/7AAD-/\pm h\text{-red}$ ), and late apoptotic or necrotic cells ( $V+/7AAD \pm h\text{-red}$ ).

Mitochondrial regulation of apoptosis and mitochondrial membrane permeability by changing the potential difference between the inner and outer parts of the membrane are closely interrelated, as has been demonstrated by a large number of research groups around the world. According to Mitchell's theory, the electrochemical potential of the proton  $\delta\Psi$ , which arises during the transfer of an electron through the inner membrane, determines the interaction of the processes of oxidation and phosphorylation, the coupling of which serves as a source of energy for the formation of adenosine triphosphate.<sup>41–43</sup>

Various changes in  $\delta\Psi$  detected by MitoSense Red dye, in combination with the externalization of phosphatidylserine to the surface of the cell membrane, are reliable signs of apoptosis due to mitochondrial damage and the formation of ROS ions. Membrane phosphatidylserine expression is assessed by annexin V binding, and plasma membrane permeability to dye 7AAD is a clear indicator of cellular apoptosis. Parallel detection of MitoSense Red dye in the presence of membrane changes with externalization of phosphatidylserine and 7AAD DNA staining is strong evidence of the detection of mitochondrial membrane damage. This multiparameter staining method is also used by many research groups around the world to detect changes in the mitochondrial membrane. It is also necessary to take into account that these processes in the cell develop in a fairly short period of time, 4 h of incubation. This is precisely the time when mitochondrial damage in the cell will ultimately initiate apoptosis via the mitochondrial pathway.

The most pronounced late apoptosis was observed when compound **6a** was added to the Jurkat cell culture, while the other two compounds **6b** and **6c** showed similar results (31.19, 24.67, and 17.15%). A comparison of the cytometric data for the synthesized macrodiolides with those for staurosporine indicates that they induced a more pronounced decrease in the mitochondrial potential. Indeed, a comparison of the percentages of cells characterized by damaged mitochondrial potential and phosphatidylserine externalization that appeared after the treatment with staurosporine and compound **6a** (Figure 1A, histogram (A)) shows that the value was 8.95% for staurosporine-treated cells and 65.34% for the cells treated with **6a**. This attests to a higher ability of macrodiolide **6a** to penetrate the mitochondrial membrane and to act apparently as an ionophore.<sup>34,44</sup> Other mechanisms of macrodiolide action on the intracellular processes such as influence on the microtubule formation or inhibition of Akt/mTOR kinase cannot be ruled out either.

To confirm mitochondrial damage, we conducted a series of experiments to detect ROS ions in cells exposed to the compounds under study. Mitochondrial regulation of apoptosis and oxidative stress are closely related, as has been demonstrated in a large number of studies.<sup>45</sup> Detection of mitochondrial stress using MitoSox Red and annexin V allows simultaneous measurement of 2 most important parameters of cell viability, the formation of mitochondrial superoxide, detected by the membrane-permeable dye MitoSox Red, and the externalization of phosphatidylserine on the cell membrane, which is assessed by the binding of this phospholipid to

annexin V in one and the same cell sample simultaneously. Multiparametric assessment of these cell viability indicators allowed us to determine the correlation and relationship of oxidative stress with apoptosis.

The highest values of oxidative stress and early apoptosis were detected in the mitochondria of cells treated with compounds **6a** (15.10%) and **6b** (15.26%). The duration of incubation with the above compounds was 4 h. Compound **6c** turned out to be less active compared to compounds **6a** and **6b** (13.05%, respectively) (Figure 1).

Analysis of the cell cycle in Jurkat cells pretreated with compounds **6a–c** demonstrated a marked decrease in the percentage of cells in the M/G2 and S phases and an increase in the percentage of cells in the G0/G1 phase compared to the control, which may indirectly attest to retardation of the cell division process due to the block at the G1/S checkpoint. Similar results were obtained in our earlier study.<sup>34</sup> Thus, apart from acting on mitochondria, the macrodiolides we prepared can apparently retard cell division by a more intricate mechanism, which is still to be studied in detail.

## CONCLUSIONS

Stereoselective syntheses of previously undescribed polyether macrodiolides containing a 1*Z*,5*Z*-diene moiety in the molecule were implemented in good yields and investigated for their antitumor activity. It was established that the resulting macrocycles exhibit cytotoxic activity in vitro against cell lines Jurkat, K562, U937, and Hek293 and are capable of inducing apoptosis of immortalized T cells (Jurkat). The compounds have been shown to affect the mitochondrial membrane through mitochondrial uncoupling and induce the production of ROS ions, as well as block the G1/S fission checkpoint. All of the above studies confirm that the synthesized macrodiolides apparently cause dissipation of mitochondrial potential and are promising drug candidates with antitumor activity.

## EXPERIMENTAL SECTION

**Materials and Methods. Chemistry.** <sup>1</sup>H, <sup>13</sup>C NMR spectra were obtained using a Bruker AVANCE 400 in CDCl<sub>3</sub> operating at 400.13 MHz for <sup>1</sup>H, 100.62 MHz for <sup>13</sup>C and Bruker Ascend-500 (500 MHz (<sup>1</sup>H)), and 125 MHz (<sup>13</sup>C)). High-resolution mass spectra of compounds were recorded on a Bruker maXis spectrometer (tandem quadrupole/time-of-flight mass analyzer) equipped with an electrospray ionization source (ESI) and matrix-activated laser desorption/ionization (MALDI). All solvents were dried and freshly distilled before use. All reactions were carried out under a dry argon atmosphere. Commercially available alkynols (Aldrich) and Cp<sub>2</sub>TiCl<sub>2</sub> (Aldrich) were used. The synthesis of compounds **6a–8f** was carried out similarly to the known procedure.<sup>40</sup> Analytical data for compounds **7a–7f** (yield, <sup>1</sup>H NMR, <sup>13</sup>C NMR, ESI-MS) are reported in the literature.<sup>46</sup>

**Biological Evaluation.** Biology studies (cell culturing, cytotoxicity assay, viability and apoptosis, cell cycle analysis, mitochondrial damage) were carried out following the known procedure.<sup>34</sup> Cells (Jurkat, K562, U937, Hek293, and Fibroblasts) were purchased from the Russian Cell Culture Collection (Institute of Cytology of the Russian Academy of Sciences, Novosibirsk, Russia) and cultured according to standard protocols and sterile technique.

**Chemical Experimental Data.** (1*OZ*,1*AZ*)-8,9,12,13,16,17,26,31-Octahydro-5*H*,20*H*-tribenzo[*c,g,k*]-

[1,5,10,14]tetraoxacyclohexacosine-7,18-dione (**6a**). White waxy solid; yield 49%.  $R_f = 0.52$ , hexane/EtOAc 5:1.  $^1\text{H NMR}$  (400 MHz,  $\text{CDCl}_3$ ):  $\delta = 7.55$  (dd,  $J = 5.2, 3.7$  Hz, 2H), 7.43–7.35 (m, 4H), 7.34–7.26 (m, 2H), 7.04–6.92 (m, 4H), 5.39–5.23 (m, 8H), 5.19 (s, 4H), 2.42–2.13 (m, 8H), 2.06–1.87 (m, 4H).  $^{13}\text{C NMR}$  (101 MHz,  $\text{CDCl}_3$ ):  $\delta = 173.1, 156.9, 134.9, 130.9, 130.5, 129.9, 128.4, 128.3, 127.9, 124.6, 120.9, 111.9, 68.1, 62.1, 34.5, 27.2, 22.8$ . ESI-MS: for  $\text{C}_{34}\text{H}_{36}\text{O}_6 + \text{Na}^+$   $[\text{M} + \text{Na}]^+$  563.2404; found 563.2412.

(13Z,17Z)-2,6,9,22-Tetraoxa-1,7(1,2),4(1,3)-tribenzenacyclotricosaphane-13,17-diene-10,21-dione (**6b**). White waxy solid; yield 56%.  $R_f = 0.55$ , hexane/EtOAc 5:1.  $^1\text{H NMR}$  (400 MHz,  $\text{CDCl}_3$ ):  $\delta = 7.53$  (s, 1H), 7.44–7.28 (m, 8H), 6.99 (dd,  $J = 8.6, 6.8$  Hz, 3H), 5.38–5.28 (m, 4H), 5.23 (s, 4H), 5.16 (s, 4H), 2.39–2.29 (m, 8H), 2.04–1.89 (m, 4H).  $^{13}\text{C NMR}$  (101 MHz,  $\text{CDCl}_3$ ):  $\delta = 173.0, 156.9, 137.4, 130.7, 130.6, 129.9, 128.7, 127.9, 126.4, 125.4, 124.7, 120.8, 111.9, 69.7, 62.3, 34.5, 27.2, 22.9$ . ESI-MS: calcd for  $\text{C}_{34}\text{H}_{36}\text{O}_6 + \text{Na}^+$   $[\text{M} + \text{Na}]^+$  563.2404; found 563.2393.

(13Z,17Z)-2,6,9,22-Tetraoxa-1,7(1,2),4(1,4)-tribenzenacyclotricosaphane-13,17-diene-10,21-dione (**6c**). White waxy solid; yield 60%.  $R_f = 0.52$ , hexane/EtOAc 5:1.  $^1\text{H NMR}$  (400 MHz,  $\text{CDCl}_3$ ):  $\delta = 7.48$  (s, 4H), 7.39–7.31 (m, 4H), 7.02–6.97 (m, 4H), 5.40–5.31 (m, 4H), 5.23 (s, 4H), 5.15 (s, 4H), 2.39–2.31 (m, 8H), 2.09–1.95 (m, 4H).  $^{13}\text{C NMR}$  (101 MHz,  $\text{CDCl}_3$ ):  $\delta = 173.1, 157.2, 136.6, 131.1, 130.6, 130.0, 129.4, 128.0, 127.2, 124.6, 120.8, 111.9, 69.7, 62.4, 34.6, 27.1, 22.9$ . ESI-MS: calcd for  $\text{C}_{34}\text{H}_{36}\text{O}_6 + \text{Na}^+$   $[\text{M} + \text{Na}]^+$  563.2404; found 563.2423.

(10Z,14Z)-8,9,12,13,16,17,26,27-Octahydro-5H,20H-dibenzo[e,w][1,4,8,21]tetraoxacyclotetracosine-7,18-dione (**6d**). White waxy solid; yield 47%.  $R_f = 0.50$ , hexane/EtOAc 3:1.  $^1\text{H NMR}$  (500 MHz,  $\text{CDCl}_3$ ):  $\delta = 7.45$ –7.30 (m, 4H), 7.05–6.92 (m, 4H), 5.49–5.31 (m, 4H), 5.20 (d,  $J = 9.1$  Hz, 4H), 4.38 (s, 4H), 2.44–2.30 (m, 8H), 2.13–2.01 (m, 4H).  $^{13}\text{C NMR}$  (126 MHz,  $\text{CDCl}_3$ ):  $\delta = 172.9, 156.5, 130.6, 129.7, 129.4, 128.2, 125.2, 121.1, 111.9, 67.0, 61.4, 34.5, 27.4, 22.8$ . ESI-MS: calcd for  $\text{C}_{28}\text{H}_{32}\text{O}_6 + \text{H}^+$   $[\text{M} + \text{H}]^+$  462.2272; found 462.2291.

(10Z,14Z)-8,9,12,13,16,17,26,27,29,30-Decahydro-5H,20H-dibenzo[h,z][1,4,7,11,24]-pentaoxacycloheptacosine-7,18-dione (**6e**). White waxy solid; yield 58%.  $R_f = 0.43$ , hexane/EtOAc 3:1.  $^1\text{H NMR}$  (500 MHz,  $\text{CDCl}_3$ ):  $\delta = 7.35$ –7.28 (m, 4H), 7.00–6.86 (m, 4H), 5.48–5.27 (m, 4H), 5.19 (d,  $J = 6.4$  Hz, 4H), 4.18 (dd,  $J = 11.6, 6.7$  Hz, 4H), 3.97 (dd,  $J = 10.7, 5.7$  Hz, 4H), 2.45–2.28 (m, 8H), 2.10–1.95 (m, 4H).  $^{13}\text{C NMR}$  (126 MHz,  $\text{CDCl}_3$ ):  $\delta = 172.9, 157.0, 130.6, 130.3, 129.7, 128.1, 124.7, 120.8, 111.8, 70.1, 68.2, 61.9, 34.5, 27.3, 22.9$ . ESI-MS: calcd for  $\text{C}_{30}\text{H}_{36}\text{O}_7 + \text{Na}^+$   $[\text{M} + \text{Na}]^+$  531.2353; found 531.2382.

(10Z,14Z)-8,9,12,13,16,17,26,27,29,30,32,33-Dodecahydro-5H,20H-dibenzo[c,k][1,4,7,10,14,27]-hexaoxacyclotriacontine-7,18-dione (**6f**). White waxy solid; yield 62%.  $R_f = 0.31$ , hexane/EtOAc 3:1.  $^1\text{H NMR}$  (500 MHz,  $\text{CDCl}_3$ ):  $\delta = 7.31$  (dd,  $J = 19.0, 8.2$  Hz, 4H), 6.99–6.87 (m, 4H), 5.48–5.30 (m, 4H), 5.18 (s, 4H), 4.19–4.16 (m, 4H), 3.91–3.88 (m, 4H), 3.78 (s, 4H), 2.45–2.27 (m, 8H), 2.14–1.95 (m, 4H).  $^{13}\text{C NMR}$  (126 MHz,  $\text{CDCl}_3$ ):  $\delta = 172.9, 157.1, 130.6, 130.4, 129.7, 128.1, 124.6, 120.7, 111.7, 71.1, 69.8, 68.2, 62.0, 34.4, 27.2, 22.9$ . ESI-MS: calcd. for  $\text{C}_{32}\text{H}_{40}\text{O}_8 + \text{Na}^+$   $[\text{M} + \text{Na}]^+$  575.2615; found 575.2624.

(13Z,17Z)-8,9,10,11,12,15,16,19,20,21,22,23,32,37-Tetra-decahydro-5H,26H-tribenzo[c,g,k][1,5,10,14]-

tetraoxacyclodotriacontine-7,24-dione (**8a**). White waxy solid; yield 55%.  $R_f = 0.58$ , hexane/EtOAc = 5:1.  $^1\text{H NMR}$  (500 MHz,  $\text{CDCl}_3$ ):  $\delta = 7.55$  (dd,  $J = 5.4, 3.5$  Hz, 2H), 7.43–7.34 (m, 4H), 7.34–7.27 (m, 2H), 7.02–6.91 (m, 4H), 5.45–5.17 (m, 12H), 2.34–2.16 (m, 4H), 2.14–1.90 (m, 8H), 1.62–1.50 (m, 4H), 1.34–1.20 (m, 8H).  $^{13}\text{C NMR}$  (126 MHz,  $\text{CDCl}_3$ ):  $\delta = 173.7, 156.7, 134.9, 130.6, 130.1, 129.8, 129.4, 128.4, 124.7, 120.9, 111.8, 68.0, 61.8, 34.2, 29.2, 28.6, 27.5, 26.9, 24.8$ . ESI-MS: calcd for  $\text{C}_{40}\text{H}_{48}\text{O}_6 + \text{Na}^+$   $[\text{M} + \text{Na}]^+$  647.3343; found 647.3357.

(16Z,20Z)-2,6,9,28-Tetraoxa-1,7(1,2),4(1,3)-tribenzenacyclononacosaphane-16,20-diene-10,27-dione (**8b**). White waxy solid; yield 60%.  $R_f = 0.55$ , hexane/EtOAc 5:1.  $^1\text{H NMR}$  (500 MHz,  $\text{CDCl}_3$ ):  $\delta = 7.54$  (d,  $J = 5.2$  Hz, 1H), 7.44–7.29 (m, 7H), 7.02–6.95 (m, 4H), 5.45–5.27 (m, 4H), 5.26–5.22 (m, 4H), 5.15 (s, 4H), 2.37–2.29 (m, 4H), 2.12–1.90 (m, 8H), 1.61 (dt,  $J = 14.4, 7.4$  Hz, 4H), 1.32–1.14 (m, 8H).  $^{13}\text{C NMR}$  (126 MHz,  $\text{CDCl}_3$ ):  $\delta = 173.7, 156.8, 137.4, 130.4, 130.0, 129.7, 129.4, 128.8, 126.6, 125.7, 124.8, 120.8, 111.9, 69.8, 61.9, 34.3, 29.2, 28.6, 27.5, 26.9, 24.8$ . ESI-MS: calcd for  $\text{C}_{40}\text{H}_{48}\text{O}_6 + \text{Na}^+$   $[\text{M} + \text{Na}]^+$  647.3343; found 647.3349.

(16Z,20Z)-2,6,9,28-Tetraoxa-1,7(1,2),4(1,4)-tribenzenacyclononacosaphane-16,20-diene-10,27-dione (**8c**). White waxy solid; yield 74%.  $R_f = 0.60$ , hexane/EtOAc = 5:1.  $^1\text{H NMR}$  (500 MHz,  $\text{CDCl}_3$ ):  $\delta = 7.47$  (s, 4H), 7.40–7.29 (m, 4H), 7.02–6.96 (m, 4H), 5.42–5.30 (m, 4H), 5.28–5.22 (m, 4H), 5.14 (s, 4H), 2.41–2.32 (m, 4H), 2.09–1.95 (m, 8H), 1.67–1.61 (m, 4H), 1.37–1.28 (m, 8H).  $^{13}\text{C NMR}$  (126 MHz,  $\text{CDCl}_3$ ):  $\delta = 173.7, 156.9, 136.6, 130.4, 130.1, 129.7, 129.4, 127.2, 124.8, 120.8, 111.9, 69.6, 61.9, 34.3, 29.2, 28.6, 27.5, 26.9, 24.8$ . ESI-MS: calcd for  $\text{C}_{40}\text{H}_{48}\text{O}_6 + \text{NH}_4^+$   $[\text{M} + \text{Na}]^+$  647.3343; found 642.3357.

(13Z,17Z)-8,9,10,11,12,15,16,19,20,21,22,23,32,33-Tetradeca-hydro-5H,26H-dibenzo[c<sub>1</sub>,e][1,4,8,27]-tetraoxacyclotriacontine-7,24-dione (**8d**). White waxy solid; yield 55%.  $R_f = 0.63$ , hexane/EtOAc 3:1.  $^1\text{H NMR}$  (500 MHz,  $\text{CDCl}_3$ ):  $\delta = 7.33$  (dd,  $J = 14.6, 7.4$  Hz, 4H), 7.03–6.93 (m, 4H), 5.47–5.31 (m, 4H), 5.19 (s, 4H), 4.38 (s, 4H), 2.31 (t,  $J = 7.5$  Hz, 4H), 2.11–1.94 (m, 8H), 1.66–1.56 (m, 4H), 1.38–1.26 (m, 8H).  $^{13}\text{C NMR}$  (126 MHz,  $\text{CDCl}_3$ ):  $\delta = 173.6, 156.6, 130.1, 129.8, 129.5, 129.4, 125.1, 121.0, 111.8, 67.0, 61.4, 34.2, 29.3, 28.7, 27.7, 26.9, 24.8$ . ESI-MS: calcd for  $\text{C}_{34}\text{H}_{44}\text{O}_6 + \text{Na}^+$   $[\text{M} + \text{Na}]^+$  571.3030; found 571.3004.

(13Z,17Z)-8,9,10,11,12,15,16,19,20,21,22,23,32,33,35,36-Hexadeca-hydro-5H,26H-dibenzo[f<sub>1</sub>,h][1,4,7,11,30]-pentaoxacyclotritriacontine-7,24-dione (**8e**). White waxy solid; yield 69%.  $R_f = 0.49$ , hexane/EtOAc 3:1.  $^1\text{H NMR}$  (500 MHz,  $\text{CDCl}_3$ ):  $\delta = 7.31$  (dd,  $J = 20.5, 8.8$  Hz, 4H), 7.01–6.87 (m, 4H), 5.47–5.28 (m, 4H), 5.19 (d,  $J = 9.5$  Hz, 4H), 4.19 (t,  $J = 4.4$  Hz, 4H), 4.00–3.92 (m, 4H), 2.34 (t,  $J = 7.3$  Hz, 4H), 2.11–1.94 (m, 8H), 1.68–1.56 (m, 4H), 1.40–1.27 (m, 8H).  $^{13}\text{C NMR}$  (126 MHz,  $\text{CDCl}_3$ ):  $\delta = 173.6, 156.9, 130.1, 129.6, 129.4, 124.9, 120.8, 111.8, 70.1, 68.2, 61.6, 34.3, 29.3, 28.7, 27.5, 26.9, 24.8$ . ESI-MS: calcd for  $\text{C}_{36}\text{H}_{48}\text{O}_7 + \text{Na}^+$   $[\text{M} + \text{Na}]^+$  615.3292; found 615.3313.

(13Z,17Z)-8,9,10,11,12,15,16,19,20,21,22,23,32,33,35,36,38,39-Octade-cahydro-5H,26H-dibenzo[i<sub>1</sub>,k][1,4,7,10,14,33]-hexaoxacyclohexatriacontine-7,24-dione (**8f**). White waxy solid; yield 72%.  $R_f = 0.35$ , hexane/EtOAc 3:1.  $^1\text{H NMR}$  (500 MHz,  $\text{CDCl}_3$ ):  $\delta = 7.37$ –7.26 (m, 4H), 7.00–6.87 (m, 4H), 5.46–5.32 (m, 4H), 5.20 (s, 4H), 4.17 (t,  $J = 4.8$  Hz, 4H), 3.89 (t,  $J = 4.7$  Hz, 4H), 2.34 (t,  $J = 7.4$  Hz, 4H), 2.11–1.95 (m,

8H), 1.69–1.60 (m, 4H), 1.41–1.30 (m, 8H).  $^{13}\text{C}$  NMR (126 MHz,  $\text{CDCl}_3$ ):  $\delta$  = 173.6, 156.9, 130.0, 129.9, 129.5, 129.4, 124.8, 120.7, 111.7, 71.1, 69.8, 68.1, 61.7, 34.3, 29.3, 28.7, 27.5, 26.9, 24.8. ESI-MS: calcd for  $\text{C}_{38}\text{H}_{52}\text{O}_8 + \text{Na}^+ [\text{M} + \text{Na}]^+$  659.3554; found 659.3573.

## ■ ASSOCIATED CONTENT

### SI Supporting Information

The Supporting Information is available free of charge at <https://pubs.acs.org/doi/10.1021/acsomega.3c09566>.

Copies of  $^1\text{H}$  NMR and  $^{13}\text{C}$  NMR spectra for compounds **6a–8f** (PDF)

## ■ AUTHOR INFORMATION

### Corresponding Authors

**Ilgiz I. Islamov** – Institute of Petrochemistry and Catalysis, Russian Academy of Sciences, Ufa 450075, Russian Federation; [orcid.org/0000-0002-7054-1369](https://orcid.org/0000-0002-7054-1369); Email: [iislamovi@gmail.com](mailto:iislamovi@gmail.com)

**Lilya U. Dzhemileva** – N. D. Zelinsky Institute of Organic Chemistry, Russian Academy of Sciences, Moscow 119991, Russian Federation; State Scientific Center of the Russian Federation Federal State Budgetary Institution, “National Medical Research Center of Endocrinology” of the Ministry of Health of the Russian Federation, Moscow 117292, Russian Federation; Email: [dzhemilev@mail.ru](mailto:dzhemilev@mail.ru)

### Authors

**Ilgam V. Gaisin** – Institute of Petrochemistry and Catalysis, Russian Academy of Sciences, Ufa 450075, Russian Federation

**Usein M. Dzhemilev** – N. D. Zelinsky Institute of Organic Chemistry, Russian Academy of Sciences, Moscow 119991, Russian Federation

**Vladimir A. D'yakonov** – N. D. Zelinsky Institute of Organic Chemistry, Russian Academy of Sciences, Moscow 119991, Russian Federation; [orcid.org/0000-0002-7787-5054](https://orcid.org/0000-0002-7787-5054)

Complete contact information is available at: <https://pubs.acs.org/doi/10.1021/acsomega.3c09566>

### Author Contributions

Conceptualization: I.I.I., V.A.D., L.U.D. and U.M.D.; methodology: I.I.I., I.V.G.; validation: I.I.I., V.A.D. and L.U.D.; investigation: I.I.I., V.A.D., L.U.D.; writing—original draft preparation: I.I.I., V.A.D., and L.U.D.; writing—review and editing: V.A.D. and L.U.D.; visualization: V.A.D.; supervision: V.A.D. and L.U.D.; project administration: V.A.D.; funding acquisition: I.I.I. All authors have read and agreed to the published version of the manuscript.

### Funding

This research was funded by the Russian Science Foundation, project no 22–73–10164.

### Notes

The authors declare no competing financial interest.

## ■ ACKNOWLEDGMENTS

The structural studies of the synthesized compounds were performed with the use of Collective Usage Centre “Agidel” of Ufa Research Center of the Russian Academy of Sciences at the Institute of Petrochemistry and Catalysis. The anticancer activity studies of the synthesized compounds were performed in Biomodule at the Laboratory of Metal Complex and

Nanoscale Catalysts of the N. D. Zelinsky Institute of Organic Chemistry of RAS.

## ■ REFERENCES

- (1) Driggers, E. M.; Hale, S. P.; Lee, J.; Terrett, N. K. The exploration of macrocycles for drug discovery - an underexploited structural class. *Nat. Rev. Drug Discovery* **2008**, *7*, 608–624.
- (2) Gruschwitz, F. V.; Klein, T.; Catrouillet, S.; Brendel, J. C. Supramolecular polymer bottlebrushes. *Chem. Commun.* **2020**, *56*, 5079–5110.
- (3) Caramori, G. F.; Østrøm, I.; Ortolan, A. O.; Nagurniak, G. R.; Besen, V. M.; Muñoz-Castro, A.; Orenha, R. P.; Parreira, R. L. T.; Galembeck, S. E. The usefulness of energy decomposition schemes to rationalize host–guest interactions. *Dalton Trans.* **2020**, *49*, 17457–17471.
- (4) Wang, X.; Jia, F.; Yang, L. P.; Zhou, H.; Jiang, W. Conformationally adaptive macrocycles with flipping aromatic sidewalls. *Chem. Soc. Rev.* **2020**, *49*, 4176–4188.
- (5) Neira, I.; Blanco-Gómez, A.; Quintela, J. M.; García, M. D.; Peinador, C. Dissecting the “Blue box”: Self-assembly strategies for the construction of multipurpose polycationic cyclophanes. *Acc. Chem. Res.* **2020**, *53*, 2336–2346.
- (6) Dale, E. J.; Vermeulen, N. A.; Juriček, M.; Barnes, J. C.; Young, R. M.; Wasielewski, M. R.; Stoddart, J. F. Supramolecular explorations: Exhibiting the extent of extended cationic cyclophanes. *Acc. Chem. Res.* **2016**, *49*, 262–273.
- (7) Hou, X. L.; You, S. L.; Tu, T.; Deng, W. P.; Wu, X. W.; Li, M.; Yuan, K.; Zhang, T. Z.; Dai, L. X. Enantioselective Transition-Metal Catalyzed Carbon–Carbon Bond Formation Reactions using Novel Chiral Ferrocenes and Cyclophanes. *Top. Catal.* **2005**, *35*, 87–103.
- (8) Guo, H.; Zhang, L. W.; Zhou, H.; Meng, W.; Ao, Y. F.; Wang, D. X.; Wang, Q. Q. Substrate-Induced Dimerization Assembly of Chiral Macrocyclic Catalysts toward Cooperative Asymmetric Catalysis. *Angew. Chem., Int. Ed.* **2020**, *59*, 2623–2627.
- (9) Gao, W. X.; Feng, H. J.; Guo, B. B.; Lu, Y.; Jin, G. X. Coordination-Directed Construction of Molecular Links. *Chem. Rev.* **2020**, *120*, 6288–6325.
- (10) Kauerhof, D.; Niemeyer, J. Functionalized Macrocycles in Supramolecular Organocatalysis. *ChemPlusChem* **2020**, *85*, 889–899.
- (11) Kotha, S.; Shirbhate, M. E.; Waghule, G. T. Selected synthetic strategies to cyclophanes. *Beilstein J. Org. Chem.* **2015**, *11*, 1274–1331.
- (12) Martins, T. P.; Rouger, C.; Glasser, N. R.; Freitas, S.; de Fraissinette, N. B.; Balskus, E. P.; Tasdemir, D.; Leão, P. N. Chemistry, bioactivity and biosynthesis of cyanobacterial alkyresorcinols. *Nat. Prod. Rep.* **2019**, *36*, 1437–1461.
- (13) Wang, Y.; Joullié, M. M. Approaches to Cyclophane-Types of Cyclopeptide Alkaloids. *Chem. Rec.* **2021**, *21*, 906–923.
- (14) Marx, L.; Lamberty, D.; Choppin, S.; Colobert, F.; Speicher, A. Atroposelective Synthesis of Isoriccardin C through a C–H Activated Heck Type Macrocyclization. *Eur. J. Org. Chem.* **2021**, *2021*, 1351–1354.
- (15) Pedersen, C. J. Cyclic polyethers and their complexes with metal salts. *J. Am. Chem. Soc.* **1967**, *89*, 2495–2496.
- (16) Pedersen, C. J. Cyclic polyethers and their complexes with metal salts. *J. Am. Chem. Soc.* **1967**, *89*, 7017–7036.
- (17) Supek, F.; Ramljak, T. S.; Marjanovic, M.; Buljubasic, M.; Kragol, G.; Ilic, N.; Smuc, T.; Zahradka, D.; Mlinaric-Majerski, K.; Kralj, M. Could LogP be a principal determinant of biological activity in 18-crown-6 ethers? Synthesis of biologically active adamantane-substituted diaza-crowns. *Eur. J. Med. Chem.* **2011**, *46*, 3444–3454.
- (18) Basok, S. S.; Schepetkin, I. A.; Khlebnikov, A. I.; Lutsyuk, A. F.; Kirichenko, T. I.; Kirpotina, L. N.; Pavlovsky, V. I.; Leonov, K. A.; Vishenkova, D. A.; Quinn, M. T. Synthesis, Biological Evaluation, and Molecular Modeling of Aza-Crown Ethers. *Molecules* **2021**, *26*, No. 2225, DOI: [10.3390/molecules26082225](https://doi.org/10.3390/molecules26082225).
- (19) Marjanović, M.; Kralj, M.; Supek, F.; Frkanec, L.; Piantanida, I.; Smuc, T.; Tusek-Bozic, L. Antitumor potential of crown ethers:



Structure-activity relationships, cell cycle disturbances, and cell death studies of a series of ionophores. *J. Med. Chem.* **2007**, *50*, 1007–1018.

(20) Arenaza-Corona, A.; Couce-Fortunez, M. D.; de Blas, A.; Morales-Morales, D.; Santillan, R.; Hopfl, H.; Rodriguez-Blas, T.; Barba, V. Further Approaches in the Design of Antitumor Agents with Response to Cell Resistance: Looking toward Aza Crown Ether-dtc Complexes. *Inorg. Chem.* **2020**, *59*, 15120–15134.

(21) Kralj, M.; Tušek-Božić, L.; Frkanec, L. Biomedical Potentials of Crown Ethers: Prospective Antitumor Agents. *Chem. Med. Chem.* **2008**, *3*, 1478–1492.

(22) Febles, M.; Montalvao, S.; Crespin, G. D.; Norte, M.; Padron, J. M.; Tammela, P.; Fernandez, J. J.; Daranas, A. H. Synthesis and biological evaluation of crown ether acyl derivatives. *Bioorg. Med. Chem. Lett.* **2016**, *26*, 5591–5593.

(23) Roy, A.; Talukdar, P. Recent Advances in Bioactive Artificial Ionophores. *ChemBioChem* **2021**, *22*, 2925–2940.

(24) Alfonso, I.; Quesada, R. Biological activity of synthetic ionophores: ion transporters as prospective drugs. *Chem. Sci.* **2013**, *4*, 3009–3019.

(25) Zhang, H.; Ye, R.; Mu, Y.; Li, T.; Zeng, H. Small Molecule-Based Highly Active and Selective K(+) Transporters with Potent Anticancer Activities. *Nano Lett.* **2021**, *21*, 1384–1391.

(26) Gokel, G. W.; Leevy, W. M.; Weber, M. E. Crown Ethers: Sensors for Ions and Molecular Scaffolds for Materials and Biological Models. *Chem. Rev.* **2004**, *104*, 2723–2750.

(27) Patel, M. B.; Garrad, E.; Meisel, J. W.; Negin, S.; Gokel, M. R.; Gokel, G. W. Synthetic ionophores as non-resistant antibiotic adjuvants. *RSC Adv.* **2019**, *9*, 2217–2230.

(28) Gokel, G. W.; Negin, S.; Cantwell, R. *Crown Ethers Comprehensive Supramolecular Chemistry*, 2nd ed.; Atwood, J. L.; W Gokel, G.; Barbour, L. J., Eds.; Elsevier Publishing Company: Amsterdam, 2017; pp 3–48.

(29) Yokoyama, T.; Mizuguchi, M. Crown ethers as transthyretin amyloidogenesis inhibitors. *J. Med. Chem.* **2019**, *62*, 2076–2082.

(30) D'yakonov, V. A.; Dzhemileva, L. U.; Dzhemilev, U. M. Natural compounds with bis-methylene-interrupted Z-double bonds: plant sources, strategies of total synthesis, biological activity, and perspectives. *Phytochem. Rev.* **2021**, *20*, 325–342.

(31) D'yakonov, V. A.; Makarov, A. A.; Dzhemileva, L. U.; Makarova, E. K.; Khusnutdinova, E. K.; Dzhemilev, U. M. The facile synthesis of the 5Z,9Z-dienoic acids and their topoisomerase I inhibitory activity. *Chem. Commun.* **2013**, *49* (75), 8401–8403.

(32) Dzhemileva, L. U.; D'yakonov, V. A.; Makarov, A. A.; Makarova, E. K.; Andreev, E. N.; Dzhemilev, U. M. Total Synthesis of Natural Lembehynone C and Investigation of Its Cytotoxic Properties. *J. Nat. Prod.* **2020**, *83*, 2399–2409, DOI: 10.1021/acs.jnatprod.0c00261.

(33) D'yakonov, V. A.; Makarov, A. A.; Dzhemileva, L. U.; Ramazanov, I. R.; Makarova, E. K.; Dzhemilev, U. M. Natural Trienoic Acids as Anticancer Agents: First Stereoselective Synthesis, Cell Cycle Analysis, Induction of Apoptosis, Cell Signaling and Mitochondrial Targeting Studies. *Cancers* **2021**, *13* (8), No. 1808, DOI: 10.3390/cancers13081808.

(34) Dzhemileva, L. U.; D'yakonov, V. A.; Islamov, I. I.; Unusbaeva, M. M.; Dzhemilev, U. M. New 1Z,5Z-diene macrodiolides: Catalytic synthesis, anticancer activity, induction of mitochondrial apoptosis, and effect on the cell cycle. *Bioorg. Chem.* **2020**, *99*, No. 103832.

(35) D'yakonov, V. A.; Dzhemileva, L. U.; Tuktarova, R. A.; Makarov, A. A.; Islamov, I. I.; Mulyukova, A. R.; Dzhemilev, U. M. Catalytic cyclometallation in steroid chemistry III: Synthesis of steroidal derivatives of 5Z,9Z-dienoic acid and investigation of its human topoisomerase I inhibitory activity. *Steroids* **2015**, *102*, 110–117.

(36) D'yakonov, V. A.; Dzhemileva, L. U.; Makarov, A. A.; Mulyukova, A. R.; Baev, D. S.; Khusnutdinova, E. K.; Tolstikova, T. G.; Dzhemilev, U. M. nZ,(n + 4)Z-Dienoic fatty acids: a new method for the synthesis and inhibitory action on topoisomerase I and Ii $\alpha$ . *Med. Chem. Res.* **2016**, *25* (1), 30–39, DOI: 10.1007/s00044-015-1446-1.

(37) Naveen, M.; Babu, S. A. Ring-closing metathesis reaction-based synthesis of new classes of polyether macrocyclic systems. *Tetrahedron* **2015**, *71* (40), 7758–7781.

(38) Ishihara, K.; Ohara, S.; Yamamoto, H. Direct Condensation of Carboxylic Acids with Alcohols Catalyzed by Hafnium(IV) Salts. *Science* **2000**, *290*, 1140–1142.

(39) de Léséleuc, M.; Collins, S. K. Direct synthesis of macrodiolides via hafnium(IV) catalysis. *Chem. Commun.* **2015**, *51*, 10471–10474.

(40) D'yakonov, V. A.; Islamov, I. I.; Dzhemileva, L. U.; Makarova, E. K.; Dzhemilev, U. M. Direct Synthesis of Polyaromatic Cyclophanes Containing Bis-Methylene-Interrupted Z-Double Bonds and Study of Their Antitumor Activity In Vitro. *Int. J. Mol. Sci.* **2021**, *22*, No. 8787, DOI: 10.3390/ijms22168787.

(41) Mitchell, P. Coupling of phosphorylation to electron and hydrogen transfer by a chemi-osmotic type of mechanism. *Nature* **1961**, *191*, 144–148.

(42) Marchetti, P.; Castedo, M.; Susin, S. A.; Zamzami, N.; Hirsch, T.; Macho, A.; Haeflner, A.; Hirsch, F.; Geuskens, M.; Kroemer, G. Mitochondrial permeability transition is a central coordinating event of apoptosis. *J. Exp. Med.* **1996**, *184*, 1155–1160.

(43) Jiang, X.; Wang, X. Cytochrome c-mediated apoptosis. *Annu. Rev. Biochem.* **2004**, *73*, 87–106.

(44) Lenz, K. D.; Klosterman, K. E.; Mukundan, H.; Kubicek-Sutherland, J. Z. Macrolides: From Toxins to Therapeutics. *Toxins* **2021**, *13*, No. 347, DOI: 10.3390/toxins13050347.

(45) Rey, F.; Ottolenghi, S.; Zuccotti, G. V.; Samaja, M.; Carelli, S. Mitochondrial dysfunctions in neurodegenerative diseases: role in disease pathogenesis, strategies for analysis and therapeutic prospects. *Neural Regen. Res.* **2022**, *17* (4), 754–758.

(46) Gaisin, I. V.; Islamov, I. I.; Dzhemileva, L. U.; Dzhemilev, U. M. Synthesis of Aromatic Macrodiolides and Study of Their Antitumor Activity In Vitro. *Chem. Proc.* **2023**, *14*, No. 59.